Sequential implication of the mental retardation proteins ARHGEF6 and PAK3 in spine morphogenesis

Roxanne Nodé-Langlois, Dominique Muller and Bernadett Boda*

Department of Basic Neuroscience, University of Geneva, School of Medicine, 1211 Geneva 4, Switzerland

*Author for correspondence (e-mail: Bernadett.Boda@medecine.unige.ch)

Accepted 21 September 2006
Journal of Cell Science 119, 4986-4993 Published by The Company of Biologists 2006
doi:10.1242/jcs.03273

Summary

The biological mechanisms underlying the mental retardation associated with mutation of the ARHGEF6 gene, a Rac1/Cdc42 exchange factor, are still unknown, although defects in the plasticity of synaptic networks have been postulated. We have cloned the rat ARHGEF6 gene and investigated, using a transfection approach, its involvement in spine morphogenesis and its relationship to p21-activated kinase 3 (PAK3). We found that expression of tagged ARHGEF6 in hippocampal slice cultures shows a punctate staining in dendritic spines that colocalizes with PSD95. Over-expression of ARHGEF6, of PAK3 or constitutively active PAK3 did not alter spine morphology. By contrast, knockdown of ARHGEF6 using a siRNA approach resulted in abnormalities in spine morphology similar to those reported with knockdown of PAK3. This phenotype could be rescued through co-expression of a constitutively active PAK3 protein, but not with wild-type PAK3. Together, these results indicate that ARHGEF6 is localized in dendritic spines where it contributes to regulate spine morphogenesis probably by acting through a downstream activation of PAK3. Similar mechanisms are thus likely to underlie the mental retardation induced by mutations of ARHGEF6 and PAK3.

Key words: Alpha-pix, Hippocampus, Postsynaptic density, siRNA, Transfection

Introduction

Over 40 X-linked mental retardation genes have been identified to date (Ropers and Hamel, 2005). Of these, four (PAK3, ARHGEF6, OPHN1 and FGD1) code for either regulators or effectors of the Rho family of small GTPases. Rho GTPases are critical regulators of the actin cytoskeleton in virtually all eukaryotic cells (Hall, 1998) where they often mediate signalling from the external environment. They play important roles in various physiological mechanisms such as cell division, migration, motility, invasion or extension of processes (Burridge and Wennerberg, 2004). In the CNS, their function has been linked to axonal growth, development of dendritic arborizations and spine morphogenesis (Govek et al., 2005). They have thus been proposed to affect the development and plasticity of brain circuits by regulating the organization and dynamics of the actin cytoskeleton (Luo, 2000; Ramakers, 2002). Recent work by different laboratories has provided evidence for a possible involvement of OPHN1 and PAK3 in the regulation of synapse formation mechanisms and/or synaptic function and plasticity (Govek et al., 2004; Boda et al., 2004; Zhang et al., 2005; Hayashi et al., 2004; Meng et al., 2005). This is consistent with other work that has shown an important role of Rac1 signalling in spine morphogenesis (Luo et al., 1996; Tashiro and Yuste, 2004; Nakayama et al., 2000; Penzes et al., 2001; Penzes et al., 2003). These data have lead to the proposition that a Rac-PAK signalling module could be activated at the synapse and contribute to synapse formation and plasticity either through a direct regulation of the actin/myosin cytoskeleton (Zhang et al., 2005) or through modulation of CREB signalling (Meng et al., 2005).

Little is known, however, about the precise mechanisms that lead to activation of this signalling module. Integrins or other adhesion molecules have been proposed as possible candidates. There are, however, a number of other regulatory molecules that might also play an important role, in particular the mental retardation gene coding for ARHGEF6 (alpha-pix or cool2), a specific guanine nucleotide exchange factor that activates Rac1 and Cdc42 (Baird et al., 2005; Kutsche et al., 2000). In addition to Rac activation, ARHGEF6 can also directly interact with PAK proteins (Manser et al., 1998; Bagrodia et al., 1999) and with the synaptic adaptor protein GIT1 (G-protein coupled receptor kinase-interacting protein 1) (Zhang et al., 2003; Zhang et al., 2005), suggesting, therefore, a possible synaptic function of the protein. However, except for general expression analyses showing a high level of expression in the brain during early embryonic development and to a lesser extent in adulthood (Kohn et al., 2004; Kutsche and Gal, 2001), very little is known about the role of ARHGEF6 in brain function. The fact that ARHGEF6 has recently been identified with PAK3 as an X-linked mental retardation gene, raises the important issue of its functional relationship with PAK3 and its possible involvement in spine morphogenesis.

We have addressed this issue and report the identification of the rat ARHGEF6 homologue, cloned from the adult rat hippocampus, and its localization in the spines of hippocampal neurons. We further show that siRNA-mediated knockdown of ARHGEF6 alters spine morphogenesis resulting in a phenotype very similar to that reported to result from suppression of PAK3. Finally, we find that the ARHGEF6 knockdown phenotype can be reversed through over-expression of an activated form of PAK3. These results provide

the first evidence for a synaptic function of ARHGEF6 in the hippocampus and a role upstream of PAK3.

Results

We started by isolating the rat ARHGEF6 homologue from the hippocampus. Primers encompassing the 5′ and 3′ coding regions and corresponding to consensus sequences of both human and mouse ARHGEF6 were used to amplify ARHGEF6 by RT-PCR using total RNA isolated from adult rat hippocampus. A PCR product of 2.3 kb was observed on DNA agarose gel (data not shown) and subcloned into a plasmid vector. Sequencing of the PCR product revealed a transcript of 2319 base pairs (GenBank: NM_001005565) with 89% and 96% homology to the human and mouse ARHGEF6 cDNA sequences, respectively. Translation of rat ARHGEF6 revealed a predicted protein of 773 amino acids, with 91% and 97% identity, respectively, to the human and mouse ARHGEF6 protein. To further examine the expression level of the ARHGEF6 gene in the hippocampus, we dissected the CA1 and CA3 pyramidal cell regions and used real time RT-PCR. Fig. 1A shows that the ARHGEF6 gene is indeed expressed in CA1-3 cell layers, although at a lower level than an isoform of CaMKII and PAK3. The expression level of ARHGEF6 is, however, comparable with that of other genes with important neuronal functions such as connexins (Weickert et al., 2005).

We next investigated the localization of ARHGEF6 in hippocampal neurons. Attempts to locate endogenous ARHGEF6 through immunohistochemistry were unsuccessful because of the unavailability of a suitable ARHGEF6 antibody. Therefore we used biolistic co-transfection to express EGFP and an N-terminal HA-tagged ARHGEF6 (HA-ARHGEF6) fusion protein in rat organotypic hippocampal slices. After 2 days of expression, slices were fixed and immunohistochemistry revealed both diffuse in the soma, and dense, punctate HA-ARHGEF6 clearly localized inside dendritic spine heads (Fig. 1B). To determine whether these puncta corresponded to regions of the spine post-synaptic density (PSD), we co-transfected the HA-ARHGEF6 and a fusion protein encoding the post-synaptic density 95 protein and GFP (PSD95-GFP) into organotypic hippocampal slice cultures. As shown in Fig. 1C, there was a marked colocalization of HA-ARHGEF6 and PSD95-GFP signals within spine heads, suggesting that ARHGEF6 is indeed present in PSDs. As a further verification for a synaptic localization of ARHGEF6, we also carried out co-immunostaining experiments for ARHGEF6-HA and synaptophysin. Fig. 1E shows that most ARHGEF6-HA puncta were closely apposed with synaptophysin-positive spots.

To analyze ARHGEF6 function, we then used an over-expression/knockdown approach through biolistic transfection of organotypic hippocampal slices. Over-expression was achieved through co-expression of various constructs together with EGFP, in order to visualize transfected neurons. For the knockdown approach, two different siRNA duplexes, specifically targeted against rat ARHGEF6 (siR1 and siR2), were engineered (Qiagen). We tested the efficiency of these siRNA in knocking down overexpressed HA-ARHGEF6 in a 3T3 fibroblast cell line, which does not contain endogenous ARHGEF6. Fibroblasts were co-transfected with the vector expressing HA-ARHGEF6 and either siR1, siR2, or a non-silencing siRNA. Western blots revealed that both siR1 and siR2 were capable of an almost total knockdown of HA-ARHGEF6 (Fig. 2A; n=3). We also verified the specificity of this effect by analyzing whether siR1 or siR2 interfered with expression of βPix, a closely related ARHGEF6 homologue, also localized in PSDs (Park et al., 2003). We found no changes in βPix expression with transfection of siR1 or siR2 in 3T3 and RAT2 cell lines (Fig. 2B). To further verify this in our model, we then also biolistically co-transfected HA-ARHGEF6 and siR1 into rat organotypic hippocampal slices.

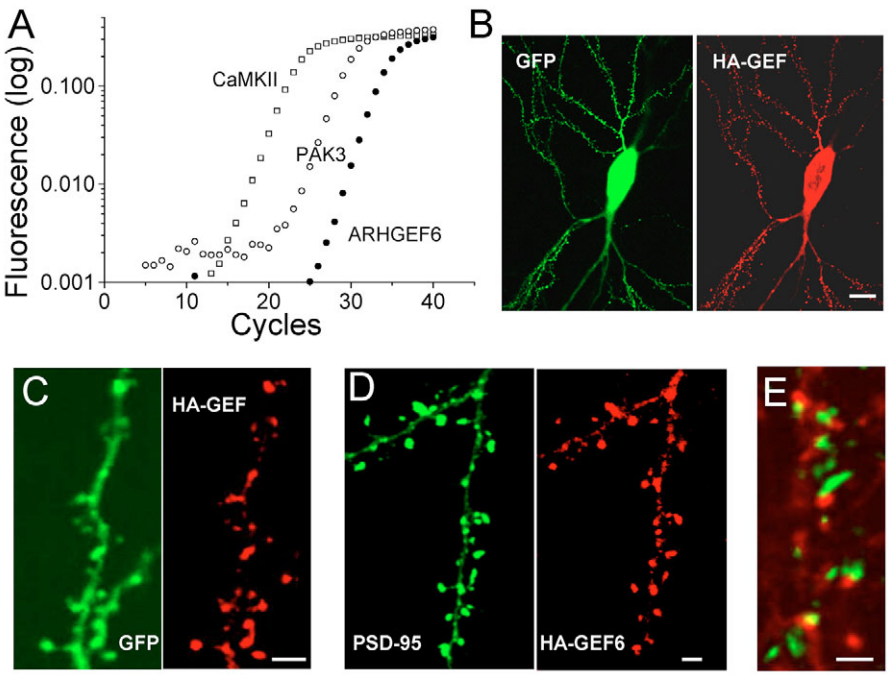

Fig. 1. Hippocampal expression of ARHGEF6 and localization in postsynaptic densities. (A) Level of expression of ARHGEF6 (filled circles), PAK3 (open circles) and CaMKII (open squares) in the CA1-3 region of the hippocampus, assessed using real-time fluorescence RT-PCR. Reverse transcription was performed with 1 μg of total RNA and a dilution corresponding to 16 ng of total RNA was amplified in a SYBRGreen PCR reaction. Data are mean of triplicate samples. (B) A pyramidal neuron co-transfected with EGFP (green, left, GFP) and HA-tagged ARHGEF6 (red, right, HA-GEF) showing a diffuse cytoplasmic and a punctate dendritic distribution of HA-ARHGEF6. (C) Magnified view of a dendritic branch obtained from a neuron co-transfected with EGFP (green, left, GFP) and HA-ARHGEF6 (red, right, HA-GEF), showing the punctate distribution at the level of spines. (D) A neuron co-transfected with PSD-95-EGFP and HA-ARHGEF6 showing the colocalization of PSD-95-EGFP puncta (PSD-95, green, left) with HA-ARHGEF6 (HA-GEF, red, right). (E) Colocalization of synaptophysin immunostaining (green) with HA-ARHGEF6 puncta (red). Bars, (B) 20 μm; (C-E) 2 μm.

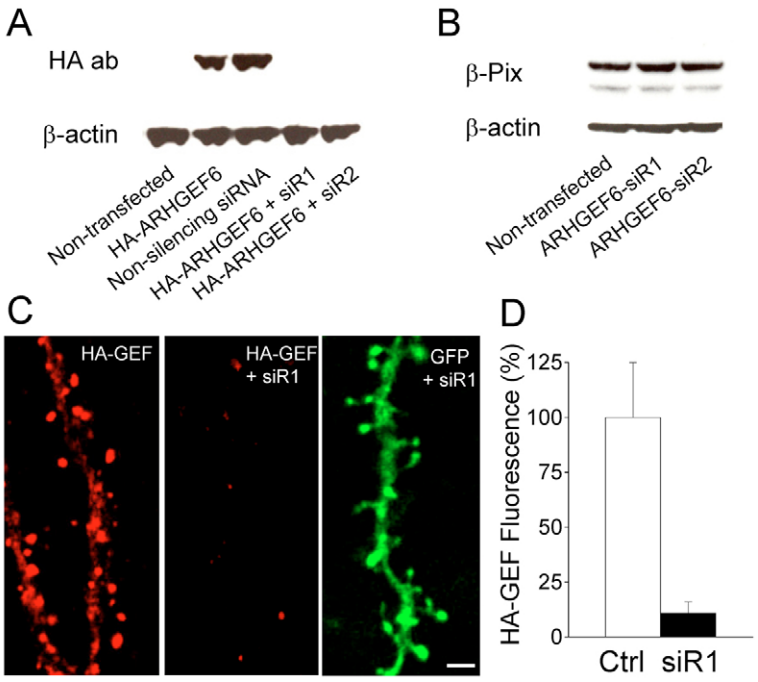

Fig. 2. Knockdown of ARHGEF6 using a siRNA transfection approach. (A) Western blot illustrating the level of expression of HA-ARHGEF6 in non-transfected fibroblasts, in fibroblasts transfected with HA-ARHGEF6, and fibroblasts co-transfected with HA-ARHGEF6 and either a non-silencing siRNA or the silencing siR1 and siR2 constructs. (B) Western blot illustrating the absence of interference of the siR1 and siR2 silencing constructs with the closely related βPix protein (weak band corresponds to a less expressed βPix isoform). (C) Punctate HA staining (red, left, HA-GEF) of a dendritic segment of a cell co-transfected with EGFP and HA-ARHGEF6, which contrasts with the HA staining (red, middle, HA-GEF + siR1) obtained from a cell co-transfected with HA-ARHGEF6, siR1 oligos and EGFP (green, right, GFP). Bar, 2 μm. (D) Quantitative analysis of HA-ARHGEF6 staining showed 89±5% reduction in siR1 co-transfected pyramidal neurons as compared to control cells. Data are mean ± s.e.m., n=4-7; P<0.05.

Immunohistochemistry showed a marked, significant reduction in the level of HA-ARHGEF6 staining in neuronal dendrites and spines in siRNA-treated cells when compared to HA-ARHGEF6-only transfected neurons (Fig. 2C; staining intensity in siRNA treated cells: 11±5% of HA-ARHGEF6 only transfected neurons; n=4-7; P<0.05; Fig. 2D).

As illustrated in Fig. 3, overexpression of the ARHGEF6 gene did not result in any detectable phenotype. The overall density of dendritic protrusions was similar in neurons co-transfected with wild-type ARHGEF6 and EGFP and in cells co-transfected with an empty vector and EGFP [0.99±0.10 spines/μm dendrite (w.t. ARHGEF6) versus 1.05±0.04 spines/μm dendrite (controls); n=6-20]. Furthermore, the proportion of stable, large mushroom type spines (defined as having a spine head diameter larger than 0.7 μm), of elongated, immature spines and of filopodia was not different in the two conditions [20.6±3.7% (w.t. ARHGEF6) vs 25.1±1.8% (controls) for mushrooms; 7.2±1.8% (w.t. ARHGEF6) vs 6.1±0.6% (controls) for long spines; 1.1±0.5% (w.t. ARHGEF6) vs 0.8±0.2% (controls) for filopodia; n=6-20]. Interestingly, this was also the case with overexpression of the wild-type PAK3 gene (21.3±3.8% for mushrooms; 4.9±1.4%, for long spines; 0.6±0.4%, for filopodia; n=5, spine density: 0.92±0.04), as well as with overexpression of a constitutively active form of PAK3 (24.7±3.3% for mushrooms; 6.7±0.5% for long spines; 0.5±0.2% for filopodia; n=12, spine density: 1±0.05; Fig. 3). Thus, neither overexpression of ARHGEF6 or PAK3 nor enhanced activity of PAK3 appeared to affect spine morphogenesis or spine density.

We then investigated how siRNA-mediated ARHGEF6 knockdown affected dendritic spines of transfected neurons. For this, hippocampal CA1 and CA3 neurons were co-transfected with siRNA (siR1, siR2 or non-silencing control siRNA) and a mammalian expression vector containing an enhanced green fluorescent protein (pcDNA-EGFP). Previous

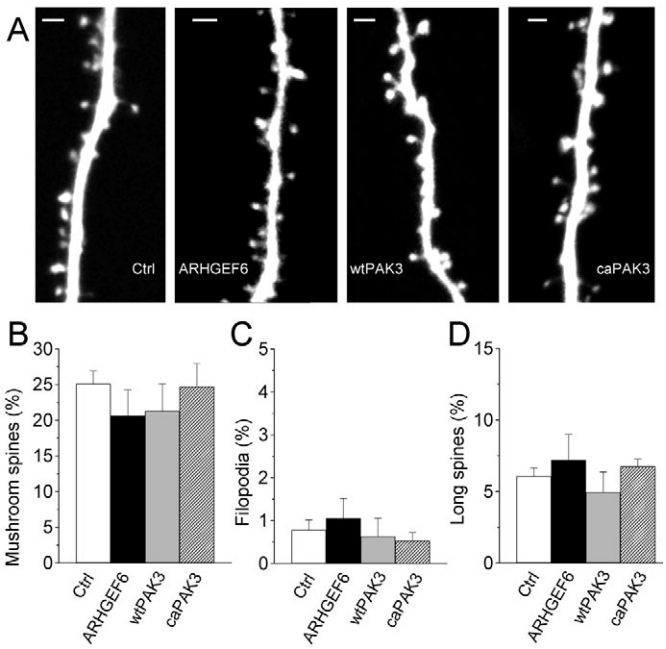

Fig. 3. Absence of spine abnormalities induced by overexpression of ARHGEF6, wild-type PAK3 or constitutively active PAK3. (A) Dendritic segments in cells transfected with EGFP (Ctrl) or co-transfected with EGFP and either wild-type ARHGEF6, wild-type PAK3 (wtPAK3) or constitutively active PAK3 (caPAK3). Bar, 2 μm. (B) Blind quantitative analysis of large mushroom-type spines (spine head diameter >0.7 μm), filopodia or elongated spines (≥1.8 μm in length) show no detectable differences between control, EGFP-transfected cells (open bars) and ARHGEF6 (black bars), wild-type PAK3 (grey bars) or constitutively active PAK3 (dashed bars) co-transfected neurons. Data are mean ± s.e.m., n=5-12.

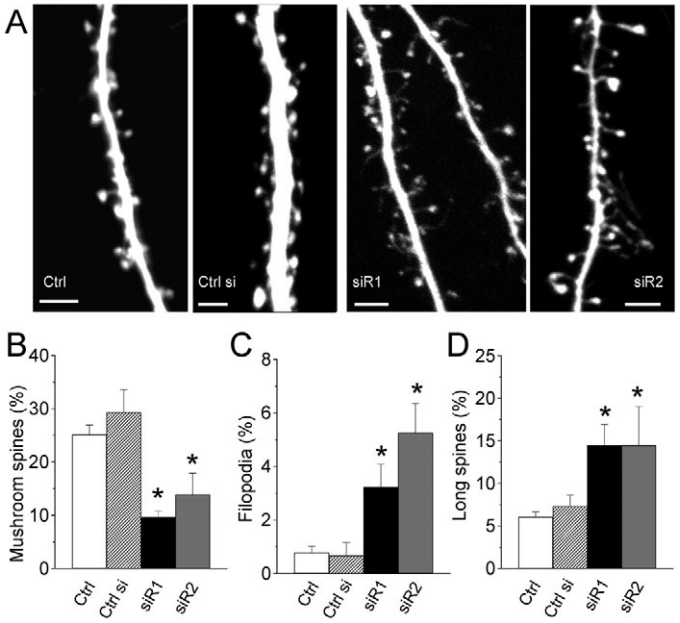

Fig. 4. Spine abnormalities induced by ARHGEF6 knockdown in hippocampal organotypic slice cultures. (A) Dendritic segments in cells transfected with EGFP (Ctrl) or co-transfected with EGFP and either a non-silencing siRNA or silencing siR1 and siR2 constructs. Note the increase in elongated spines and filopodia. Bar, 3 μm. (B) Blind quantitative analysis of large mushroom-type spines (spine head diameter >0.7 μm) shows a significant reduction in siR1 (dark grey bar) and siR2 (grey bar) transfected cells versus EGFP-transfected control neurons (white bar) or non-silencing siRNA transfected cells. (C) Increase in filopodia observed under the same experimental conditions. (D) Increase in elongated spines (⩾1.8 μm). Data are mean ± s.e.m., n=6-20; *P<0.05.

work and new experiments with different tagged proteins have shown the efficiency of this co-transfection approach (Boda et al., 2004). Transfected cells were then analyzed using live confocal imaging. With both siR1 and siR2 transfections, we observed a characteristic phenotype with regard to spine morphology. With the exception of a few cells in which transfection did not result in clearly observable differences from control neurons, most transfected cells (10 out of 14 siR1 and 6 out of 9 siR2 transfected cells) revealed marked alterations of dendritic spine morphology (Fig. 4A). Blind morphometric analysis of siR1- and siR2-transfected cells was then carried out on a total of 2029, 1074 and 1177 protrusions from 20 control (non-silencing siRNA or EGFP cells), six siR1 and six siR2 phenotypic transfected neurons, respectively. These analyses revealed no changes in spine density (0.99±0.08 spines/μm dendrite, siR1, and 0.99±0.06 spines/μm dendrite, siR2 vs 1.05±0.04 spines/μm dendrite, controls), but marked differences in the morphology or type of protrusions. There was a marked decrease in large, mushroom-type spines (8.8±1.5% siR1, and 13.9±4.0% siR2 vs 25.1±1.8% (controls); P<0.05; n=6-20; Fig. 2B-D), a clear increase in the proportion of filopodia (2.5±0.9% siR1, and 5.3±1.1% siR2 vs 0.8±0.2%, controls; P<0.05) and of elongated spines (12.2±3.3% siR1, and 14.5±4.5% siR2, vs 6.1±0.6% controls; P<0.05; Fig. 4B-D). Overall, considering all protrusions analyzed, the mean size of spine heads significantly decreased by about 10-15% in siRNA-transfected cells (from 0.63±0.01 μm in control cells to 0.54±0.02 μm in siR1 and 0.57±0.02 μm in siR2-transfected cells, n=6-20; P<0.05), whereas the mean length of protrusions increased by about 15-20% (1.06±0.02 μm in control cells vs 1.23±0.11 μm in SiR1 and 1.33±0.10 μm in siR2-transfected neurons, n=6-20; P<0.05).

As this phenotype clearly reproduced the one recently described upon suppression of PAK3 (Boda et al., 2004), and as ARHGEF6 has been suggested to act as an activator of the Rac-PAK cascade (Daniels et al., 1999; Baird et al., 2005; Zhang et al., 2005) and/or directly bind to PAK proteins (Manser et al., 1998; Bagrodia et al., 1999), we explored the possibility of an interaction between ARHGEF6 and PAK3 signalling for this phenotype. In particular, we investigated whether an activated form of the kinase was capable of reversing the phenotype produced by siRNA-mediated ARHGEF6 knockdown in hippocampal neurons. A PAK3 mutant carrying three separate single nucleotide substitutions in its Cdc42/Rac1 binding domain rendering it constitutively active (caPAK3) (Bagrodia et al., 1995) was biolistically co-transfected in hippocampal slices with the pcDNA-EGFP and ARHGEF6 siRNAs. Blind analysis of spine characteristics under these conditions showed that co-expression of constitutively active PAK3 with ARHGEF6 siR1 completely prevented the appearance of the ARHGEF6 knockdown phenotype (n=8). As illustrated in Fig. 5A and quantified in Fig. 5B, the proportion of filopodia (0.2±0.1%), elongated spines (5.5±1.5%) or large mushroom spines (25.0±2.4%) was similar in caPAK3-siR1-transfected cells as in the control, non silencing siRNA or EGFP-transfected neurons (0.8±0.2% filopodia; 6.1±0.6% long spines; 25.1±1.8% mushroom spines; n=8-20; P>0.2). By contrast, cells transfected with ARHGEF6 siR1 oligos (n=10), ARHGEF6 siR1 oligos and an empty vector (n=3) or ARHGEF6 siR1 oligos and wild-type PAK3 (n=9) showed the characteristic ARHGEF6 knockdown phenotype (Fig. 5). As mentioned above, expression of caPAK3 alone did not affect spine morphology (0.5±0.2% filopodia; 6.7±0.5% long spines; 24.7±3.3% mushroom spines; n=12) or density. The changes observed upon transfection with ARHGEF6 siRNAs, characterized by a reduction of large mushroom-type spines and an increase in elongated spines, were therefore reversed upon co-transfection with constitutively active PAK3, but not with wild-type PAK3.

In additional experiments, we then also analyzed the effects of double knockdown of ARHGEF6 and PAK3 using co-transfection with ARHGEF6 SiR1 and a specific PAK3 siRNA (Boda et al., 2004). As illustrated in Fig. 6, the double knockdown of PAK3 and ARHGEF6 (siGEF+siPAK3, black bar) showed a very similar phenotype to the one reported with the single knockdown (siGEF, dashed bar). Furthermore, this particular phenotype, when produced by PAK3 knockdown, could not be rescued by over-expression of wild-type ARHGEF6 (siPAK3 + wtGEF, grey bar). These results, thus, further support the interpretation that ARHGEF6 affects spine morphogenesis probably by acting upstream of PAK3.

Discussion

In this work we identified the mental retardation gene ARHGEF6 as an additional important regulator of spine morphogenesis. We first cloned the rat homologue of

ARHGEF6. We then showed that expression of HA-tagged ARHGEF6 selectively stains dendritic spines and specifically colocalizes with PSD-95 and other synaptic proteins in hippocampal slice cultures, indicating that ARHGEF6 is a likely constituent of PSD complexes, as is βPix, another closely related member of this family of protein, also detected at excitatory synaptic sites in cultured neurons (Park et al., 2003). We further show that ARHGEF6 is required for spine morphogenesis, as suppression of ARHGEF6 resulted in general alterations of spine morphology characterized by a decrease of large mushroom-type spines and an increase of elongated spines and filopodia-like protrusions. This effect is likely to be related to a lack of downstream activation of PAK3 as, firstly, it closely resembles the phenotype recently reported following suppression of PAK3 or expression of mutated, dominant-negative forms of PAK3 (Boda et al., 2004) and, secondly, it could be rescued by a constitutively active form of PAK3, but not by wild-type PAK3. This interpretation is further supported by the fact that the double knockdown of ARHGEF6 and PAK3 still exhibit the same phenotype, whereas, by contrast, knockdown of PAK3 cannot be rescued by over-expression of ARHGEF6. Together these results strongly suggest that ARHGEF6 is involved in the same signalling module as PAK3, thereby regulating spine morphogenesis and plasticity of synaptic networks.

Interestingly, this characteristic phenotype is also very

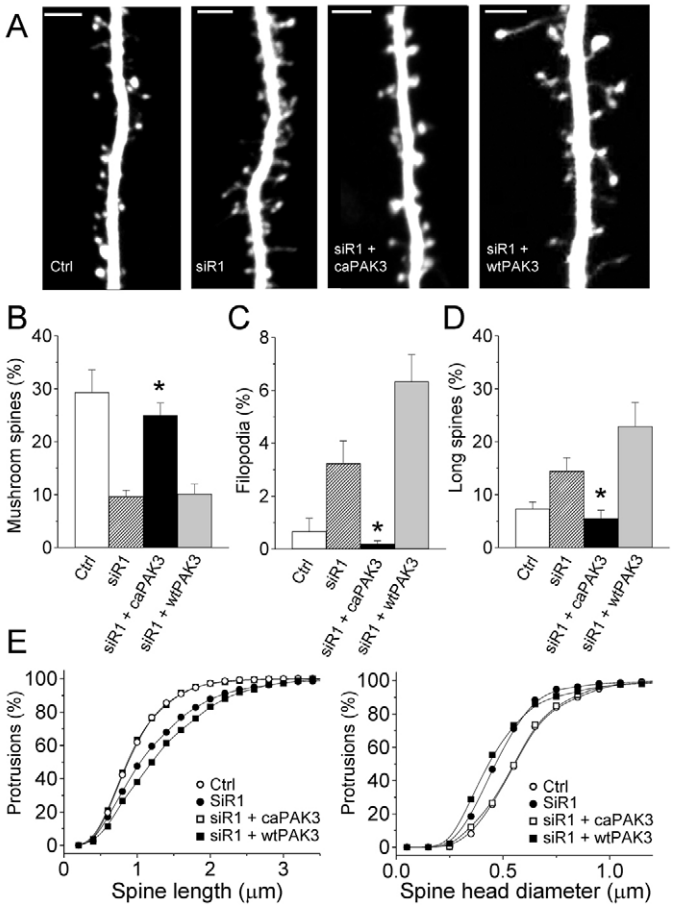

Fig. 5. Co-transfection with constitutively active PAK3, but not wild-type PAK3 rescues the phenotype induced by ARHGEF6 knockdown. (A) Illustration of dendritic segments obtained from pyramidal neurons transfected with EGFP (Ctrl), a silencing siR1 construct (siR1), a siR1 construct together with constitutively active PAK3 (siR1 + caPAK3), or a siR1 construct together with wild-type PAK3 (siR1 + wtPAK3). Note the reversal of the ARHGEF6 phenotype by caPAK3, but not wtPAK3. Bar, 3 μm. (B) Blind quantitative analysis of spine parameters show that the decrease in large mushroom-type spines induced by siR1 transfection (dashed bar) is reversed by co-transfection with constitutively active PAK3 (black bar), but not with wild-type PAK3 (grey bar). Data are mean ± s.e.m., n=8-20; *P<0.05). (C,D) Same as in B, but with regard to proportion of filopodia and elongated spines (≥1.8 μm; n=8-20; *P<0.05). (E) Cumulative distribution plot of the spine lengths and spine head diameters measured under control conditions (open circles), in siR1 transfected cells (filled circles), in cells co-transfected with siR1 and constitutively active PAK3 (open squares) and in cells co-transfected with siR1 and wild-type PAK3 (filled squares).

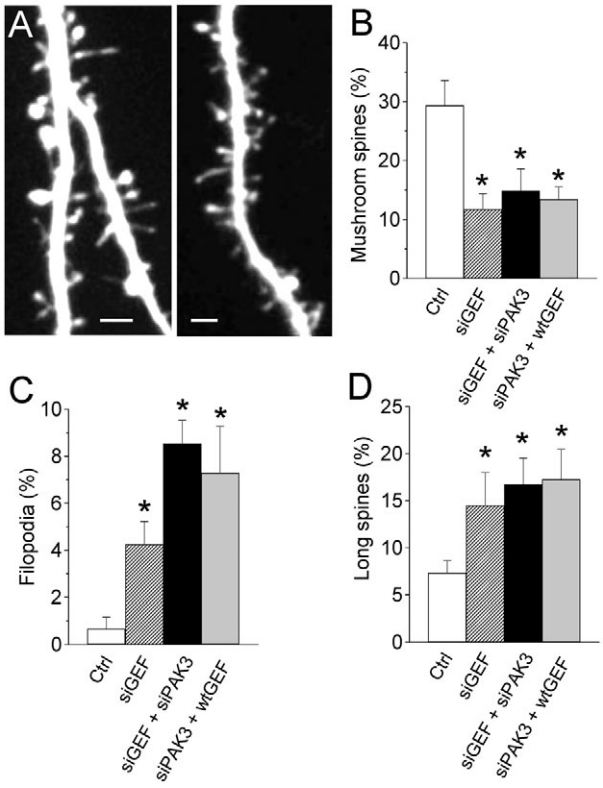

Fig. 6. Effects of double knockdown and reverse rescue experiments between ARHGEF6 and PAK3. (A) The abnormal phenotype obtained in a cell co-transfected with EGFP, ARHGEF6 siR1 and PAK3 siRNA (left) and in a cell co-transfected with EGFP, PAK3 siRNA and wild-type ARHGEF6 (right). Bar, 2 μm. (B) Changes in large mushroom-type spines (spine head diameter >0.7 μm) observed in control, EGFP-transfected cells (white bar), in ARHGEF6 siRNA transfected cells (siGEF, dashed bar), in double knockdown cells transfected with EGFP, ARHGEF6 siR1 and PAK3 siRNA (siGEF + siPAK3, black bar), and in reversed rescue experiments (cells transfected with EGFP, PAK3 siRNA and wild-type ARHGEF6; siPAK3 + wtGEF, grey bar). Data are mean ± s.e.m. of 5-11 cells; *P<0.05. (C) Same as in B, but for filopodia. (D) Same as in B, but for elongated spines (≥1.8 μm).

analogous to that reported in mentally retarded patients and in cases of fragile X mental retardation (Irwin et al., 2001; Purpura, 1974). It was observed in most transfected cells, with, however, some variability that was probably related to variations in the level of ARHGEF6 knockdown that could be obtained through siRNA transfection. The specificity of these results is indicated by several observations: (1) the abnormal phenotype was reproduced by the two ARHGEF6 siRNAs tested, but not by a scrambled one and not by other transfections that did not alter ARHGEF6 or PAK3 signalling; (2) the siRNAs used specifically targeted ARHGEF6 and PAK3 without affecting closely related proteins such as βPix or PAK1 and PAK2 (Boda et al., 2004); (3) the rescue experiments, which are consistent with a sequential involvement of ARHGEF6 and PAK3, add further indications for alteration of a specific signalling pathway.

The phenotype reported here is also consistent with the alterations in spine morphology observed following molecular interference with either kalirin, the Rho GTPase Rac or PAKs (Ma et al., 2003; Nakayama et al., 2000; Tashiro and Yuste, 2004; Zhang et al., 2005) in dissociated hippocampal cell cultures. As a general feature, blockade of Rac1 or PAKs function has been found to be associated with the appearance of thin, long spines and an inhibition of spine head growth, morphing, and stability (Tashiro and Yuste, 2004; Boda et al., 2004), whereas increased activity of PAKs resulted in an increase in protrusion density (Zhang et al., 2005). Curiously, we did not observe changes in protrusion density following over-expression of ARHGEF6 or PAK3, or even with constitutively activated PAK3 in slice cultures. It might be that the higher density of spines and synapses in slice cultures compared to dissociated cultures and their more complex environment, closer to the in vivo situation, imposes different constraints and regulations that minimize these changes. Similarly the results obtained with transfection are somewhat at variance with those obtained in transgenic mice models. Mice deficient in PAK3 or PAKs were reported to exhibit little morphological or functional abnormalities (Meng et al., 2005; Hayashi et al., 2004), although the results still suggested defects in synaptic plasticity. These variations might eventually be accounted for by the fact that the defects might be more specifically expressed during certain phases of brain development, or by compensation mechanisms, more likely to occur in transgenic animals. Although it is not yet clear how, the different PAK proteins might in fact compensate for each other, as their structures and kinase activity share many similarities (Hofmann et al., 2004). One possibility is that the specificity between members of the PAK family comes from their subcellular localization and association with specific protein complexes, rather than their activity.

In this regard, an interesting finding of this study is that the phenotype induced by ARHGEF6 knockdown could be rescued by expression of constitutively active PAK3, but not wild-type PAK3. This clearly suggests that ARHGEF6 acts upstream of PAK3, but also, as wild-type PAK3 was ineffective, that PAK3-mediated phosphorylation activity is a critical step in the signalling cascade. The fact that, conversely, the effects of PAK3 knockdown could not be rescued by ARHGEF6 over-expression and that double knockdown of PAK3 and ARHGEF6 still reproduced the same phenotype, further add to this interpretation. It should be made clear, however, that we cannot exclude that other PAK proteins, such as PAK1, might also be involved and contribute. Together, these results are consistent with the proposition of existence of a signalling module involving GIT1, Rac1, PAK3 and ARHGEF6 located in dendritic spines (Zhang et al., 2005). The function of this module might be to regulate the dynamics of the actin cytoskeleton and/or, as suggested by a recent study of PAK3 knockout mice, the MAP kinase pathway and the level of phosphorylated CREB (Meng et al., 2005). By being involved in this signalling module, ARHGEF6 might contribute to the regulation of the morphological spine rearrangements and/or the mechanisms of protein synthesis that underlie the maturation and stabilization of functional synapses. A defect in this process might thus account both for the reduced number of stable, mushroom-type spines and for the increase in filopodia and elongated, immature spines observed in the present study. Such a mechanism might interfere with the properties of plasticity that allow refinement, pruning and stabilization of synaptic networks and thereby eventually account for the cognitive defects associated with mutation of both ARHGEF6 and PAK3. Additional work will be required to better understand how and when synaptic functions are affected, but the present study provides the first evidence that ARHGEF6 indeed acts in concert with PAK3 in dendritic spines to regulate their morphogenesis. Therefore, these results strongly suggest that common mechanisms might underlie these two genetic forms of mental retardation.

Materials and Methods

RT-PCR

Total RNA was isolated from 70 mg of adult rat hippocampus using TRIzol^{R} Reagent (Invitrogen, San Diego, CA, USA) according to the manufacturer's instructions. For first-strand cDNA synthesis, 2 μg of total RNA was reverse transcribed using Superscript^{TM} II Reverse transcriptase (Invitrogen). 2 μl of the first-strand reaction was taken as template in a PCR reaction using Pfx polymerase (Invitrogen; primer sequences: 5′CAT GAA TCC AGA AGA ACG CGT T3′ and 5′TTA CTG AAG AAT CGA GGT CTT GCT3′). The A-Addition Kit (Qiagen, Hilden, Germany) was used to add single 3′deoxyadenosine overhangs to the PCR product, which was then cloned into the pcDNA3.1/V5-His TOPO^{R} TA Expression vector (Invitrogen). The PCR inserts were sequenced using an ABI Prism 3100 Genetic Analyzer (Applied Biosystems, Foster City, CA, USA). For fluorescence real-time RT-PCR, the CA1 and CA3 regions of the hippocampus were dissected and total RNA extracted. 1 μg of total RNA was reverse transcribed using Superscript^{TM} II reverse transcriptase (Invitrogen) with oligo(dT) primers, and cDNA was serially diluted and cycled in triplicate to obtain a standard curve of PCR efficiency. Primers: 5′ TGC CTG GCT CGG TGG AGA AGT AT 3′ and 5′ CAG AAC CTT GGA GAA ATT GGC CC 3′ for ARHGEF6; 5′ TAC CCA CCT TTC TGG GAT GAG 3′ and 5′ GTG GTC TGT CTG CCC ACT GAG 3′ for CAMKIIb; 5′ AGC AAT GGG CAC GAC TAC TCC 3′ and 5′ TGG TCT TGG TGC AAT GAC AGG 3′ for PAK3, were used with iQ SYBR Green Supermix (Bio-Rad, Hercules, CA, USA) according to the manufacturer's instructions in an iCycler machine (Bio-Rad). All primers generated a single amplicon as determined by the dissociation curve analysis and the PCR efficiencies (E=10exp−1/slope) were all between 2 and 1.97, allowing for relative comparison.

Constructs and siRNAs

pcDNA3.1 plasmids were used to code for EGFP (enhanced green fluorescent protein) and the PAK3 constructs (kindly provided by C. A. Walsh, Harvard Medical School, Boston, MA, USA): wild-type PAK3 (wtPAK3) and constitutively activated PAK3 (caPAK3) containing the F91S, G93A and P95A mutations in its Cdc42/Rac binding domain (Bagrodia et al., 1995). For the immunohistochemistry experiments, we used a pMT2smHA vector coding for an N-terminal HA-tagged wild-type ARHGEF6 (HA-ARHGEF6) (a gift from K. Kutsche, Institut fur Humangenetik, Universitatsklinikum Hamburg-Eppendorf, Hamburg, Germany) and a C-terminal PSD95-GFP fusion construct encoded in the GW1 mammalian expression vector (a gift from D. S Bredt, Department of Physiology, University of California, San Francisco, CA, USA). siRNAs (HiPerformance 2-For-Silencing duplexes) were

obtained from Qiagen. Target sequences for ARHGEF6 were 5′ CTG GCT TAC TGT GCA AAT CAT3′ (siR1) and 5′AAG TCA CCA GTT GAT AGT AAA 3′ (siR2). Both sequences resulted in a similar phenotype. PAK3 targeting sequence was 5′ TAG CAG CAC ATC AGT CGA ATA 3′. The sequence used as non-silencing siRNA control was 5′AAT TCT CCG AAC GTG TCA CGT 3′.

Cell line transfections and immunoblots

Mouse NIH 3T3 fibroblasts were maintained in DMEM supplemented with 10% foetal calf serum and penicillin-streptomycin. Rat RAT2 fibroblasts were cultured in DMEM supplemented with 5% foetal bovine serum and penicillin-streptomycin. Cells were co-transfected with HA-ARHGEF6 and one of either siR1 or siR2 or the non-silencing siRNA (as control), at 90% confluence using Lipofectamine 2000 (Invitrogen). The fibroblasts were harvested 48 hours post-transfection, and total protein was extracted using a triple detergent (1% Nonidet P-40, 1% sodium cholate, 0.05% SDS, 20 mM Tris, pH 7.5, 100 mM NaCl and protease inhibitor (Complete Protease Inhibitor Cocktail; Roche, Rotkreuz, Switzerland). Proteins from whole-cell lysates (30 μg) were separated by SDS-PAGE (NuPAGE^{TM}, Invitrogen) and transferred to nitrocellulose membrane (Bio-Rad). Membranes were rinsed in phosphate-buffered saline (PBS) complemented with 0.2% Tween 20, and then blocked in 5% powdered milk. Blots were then incubated with HA-TAG 6E2 mouse antibody at 1:1000 (Cell Signalling Technology, Beverly, MA, USA), βPix rabbit polyclonal antibody at 1:2000 (Chemicon, Temecula, CA, USA) and anti-β-actin mouse antibody at 1:10000 (Sigma-Aldrich, Buchs, Switzerland) overnight at 4°C, rinsed, and incubated for 1 hour at room temperature with anti-mouse and anti-rabbit IgG HRP conjugates (Bio-Rad) before detection using enhanced chemiluminescence (ECL; Amersham Biosciences, Freiburg Germany).

Organotypic cultures and biolistic transfections

Rat organotypic hippocampal slice cultures were prepared as described previously (Stoppini et al., 1991). Cultures were maintained for 11-12 days in vitro and transfected using the gene gun (Bio-Rad) technique according to the manufacturer's instructions. For the knockdown experiments, 40 μg siRNA duplex and 20 μg pcDNA3.1-EGFP were co-precipitated onto 10 mg of 1.6 μm gold beads. For the rescue experiments, 40 μg pcDNA3.1-PAK3-CA or empty vector, 20 μg pcDNA3.1-EGFP and 40 μg siRNA1 were used. Transfection of 5-20 cells per slice culture was reproducibly obtained, and expression was transient between 24 and 96 hours, with a peak at 48 hours. Control experiments showed that cells co-transfected with EGFP and pDsRed constructs expressed green and red fluorescence in all cases (n=7). Similarly co-transfection of PSD-95-EGFP and DsRed (n=10), HA-ARHGEF6 and EGFP (n=5) or HA-ARHGEF6 and PSD95-EGFP (n=8) showed co-staining in all cases, except one negative example, indicating a very good efficacy of co-transfection.

For immunohistochemistry, slice cultures were fixed at 2 days post-transfection with a fixative containing 4% formaldehyde, 75 mM lysine, 10 mM sodium periodate at 4°C for 40 minutes. Slices were washed three times with PBS, blocked with 3% bovine serum albumin (BSA) in PBS and 0.2% Triton X-100 for 1.5 hours, and then incubated for 48 hours with a primary monoclonal mouse anti-HA antibody (Cell Signalling Technology; 1:100 in PBS, 3% BSA and 0.2% Triton X-100). Cultures were rinsed three times in PBS and incubated with goat anti-mouse Cy3-conjugated secondary antibody (Jackson ImmunoResearch, West Grove, PA, USA; 1:1000 in PBS) for 2 hours. After three washes, slices were mounted on glass slides with FluorSave medium (Calbiochem, La Jolla, CA, USA) and imaged with an LSM510 confocal microscope (Zeiss, Oberkochen, Germany). For double immunohistochemistry of HA and synaptophysin antibodies, we fixed the slices with 4% paraformaldehyde at 4°C for 1 hour and in 100% methanol at –20°C for 5 minutes. Rabbit monoclonal anti-synaptophysin antibody was diluted 1:250 (Abcam, Cambridge, UK) and revealed by Alexa Fluor 488 goat anti-rabbit IgG (Invitrogen).

Image acquisition and analysis

Two days after transfection, hippocampal organotypic cultures were submerged in a chamber perfused with an extracellular medium containing the following (in mM): 124 NaCl, 1.6 KCl, 2.5 $CaCl_2$, 1.5 $MgCl_2$, 24 $NaHCO_3$, 1.2 KH_2PO_4, 10 glucose, and 2 ascorbic acid, pH 7.4 (saturated with 95% O_2 and 5% CO_2 at 33°C). Dendritic segments were imaged using a Visitron (Puchheim, Germany) spinning-disk confocal system. Control experiments showed that repetitive imaging under those conditions did not affect the morphology or viability of transfected cells. Z-stacks of 50- to 200-μm-long dendritic segments were taken of secondary and tertiary dendrites of CA1 and CA3 pyramidal neurons, and the characteristics of dendritic protrusions were measured using NIH Image MetaMorph software. The parameters analyzed included protrusion density and length (measured from the limit of the dendrite to the tip of the protrusion) and size of spine head (taken as the larger diameter). All spine measurements were made blind on individual Z-stack images of dendritic segments without corrections for z-axis projection and without introducing any threshold. Dendritic protrusions were defined as follows: filopodia (length ⩾1.8 μm, without head enlargement), long spines (length ⩾1.8 μm) and mushroom spines (spine head diameter ⩾0.7 μm).

We thank C. A. Walsh and A. Chenn for providing the PAK3, K. Kutsche for ARHGEF6 constructs and L. Parisi-Jourdain and M. Moosmayer for excellent technical support. This work was supported by grant 31-105721 from the Swiss Science Foundation, Desirée and Nils Yde's Foundation, Jérôme Lejeune Foundation, Jules Thorn Charitable Trust, Swiss Telethon Foundation, Eagle Foundation and European Synscaff project.

References

Bagrodia, S., Derijard, B., Davis, R. J. and Cerione, R. A. (1995). Cdc42 and PAK-mediated signalling leads to Jun kinase and p38 mitogen-activated protein kinase activation. *J. Biol. Chem.* **270**, 27995-27998.

Bagrodia, S., Bailey, D., Lenard, Z., Hart, M., Guan, J. L., Premont, R. T., Taylor, S. J. and Cerione, R. A. (1999). A tyrosine-phosphorylated protein that binds to an important regulatory region on the cool family of p21-activated kinase-binding proteins. *J. Biol. Chem.* **274**, 22393-22400.

Baird, D., Feng, Q. and Cerione, R. A. (2005). The Cool-2/alpha-Pix protein mediates a Cdc42-Rac signalling cascade. *Curr. Biol.* **15**, 1-10.

Boda, B., Alberi, S., Nikonenko, I., Node-Langlois, R., Jourdain, P., Moosmayer, M., Parisi-Jourdain, L. and Muller, D. (2004). The mental retardation protein PAK3 contributes to synapse formation and plasticity in hippocampus. *J. Neurosci.* **24**, 10816-10825.

Burridge, K. and Wennerberg, K. (2004). Rho and Rac take center stage. *Cell* **116**, 167-179.

Daniels, R. H., Zenke, F. T. and Bokoch, G. M. (1999). alphaPix stimulates p21-activated kinase activity through exchange factor-dependent and -independent mechanisms. *J. Biol. Chem.* **274**, 6047-6050.

Govek, E. E., Newey, S. E., Akerman, C. J., Cross, J. R., Van der Veken, L. and Van Aelst, L. (2004). The X-linked mental retardation protein oligophrenin-1 is required for dendritic spine morphogenesis. *Nat. Neurosci.* **7**, 364-372.

Govek, E. E., Newey, S. E. and Van Aelst, L. (2005). The role of the Rho GTPases in neuronal development. *Genes Dev.* **19**, 1-49.

Hall, A. (1998). Rho GTPases and the actin cytoskeleton. *Science* **279**, 509-514.

Hayashi, M. L., Choi, S. Y., Rao, B. S., Jung, H. Y., Lee, H. K., Zhang, D., Chattarji, S., Kirkwood, A. and Tonegawa, S. (2004). Altered cortical synaptic morphology and impaired memory consolidation in forebrain-specific dominant-negative PAK transgenic mice. *Neuron* **42**, 773-787.

Hofmann, C., Shepelev, M. and Chernoff, J. (2004). The genetics of Pak. *J. Cell Sci.* **117**, 4343-4354.

Irwin, S. A., Patel, B., Idupulapati, M., Harris, J. B., Crisostomo, R. A., Larsen, B. P., Kooy, F., Willems, P. J., Cras, P., Kozlowski, P. B. et al. (2001). Abnormal dendritic spine characteristics in the temporal and visual cortices of patients with fragile-X syndrome: a quantitative examination. *Am. J. Med. Genet.* **98**, 161-167.

Kohn, M., Steinbach, P., Hameister, H. and Kehrer-Sawatzki, H. (2004). A comparative expression analysis of four MRX genes regulating intracellular signalling via small GTPases. *Eur. J. Hum. Genet.* **12**, 29-37.

Kutsche, K. and Gal, A. (2001). The mouse Arhgef6 gene: cDNA sequence, expression analysis, and chromosome assignment. *Cytogenet. Cell Genet.* **95**, 196-201.

Kutsche, K., Yntema, H., Brandt, A., Jantke, I., Nothwang, H. G., Orth, U., Boavida, M. G., David, D., Chelly, J., Fryns, J. P. et al. (2000). Mutations in ARHGEF6, encoding a guanine nucleotide exchange factor for Rho GTPases, in patients with X-linked mental retardation. *Nat. Genet.* **26**, 247-250.

Luo, L. (2000). Rho GTPases in neuronal morphogenesis. *Nat. Rev. Neurosci.* **1**, 173-180.

Luo, L., Hensch, T. K., Ackerman, L., Barbel, S., Jan, L. Y. and Jan, Y. N. (1996). Differential effects of the Rac GTPase on Purkinje cell axons and dendritic trunks and spines. *Nature* **379**, 837-840.

Ma, X. M., Huang, J., Wang, Y., Eipper, B. A. and Mains, R. E. (2003). Kalirin, a multifunctional Rho guanine nucleotide exchange factor, is necessary for maintenance of hippocampal pyramidal neuron dendrites and dendritic spines. *J. Neurosci.* **23**, 10593-10603.

Manser, E., Loo, T. H., Koh, C. G., Zhao, Z. S., Chen, X. Q., Tan, L., Tan, I., Leung, T. and Lim, L. (1998). PAK kinases are directly coupled to the PIX family of nucleotide exchange factors. *Mol. Cell* **1**, 183-192.

Meng, J., Meng, Y., Hanna, A., Janus, C. and Jia, Z. (2005). Abnormal long-lasting synaptic plasticity and cognition in mice lacking the mental retardation gene Pak3. *J. Neurosci.* **25**, 6641-6650.

Nakayama, A. Y., Harms, M. B. and Luo, L. (2000). Small GTPases Rac and Rho in the maintenance of dendritic spines and branches in hippocampal pyramidal neurons. *J. Neurosci.* **20**, 5329-5338.

Park, E., Na, M., Choi, J., Kim, S., Lee, J.-R., Yoon, J., Park, D., Sheng, M. and Kim, E. (2003). The Shank family of postsynaptic density proteins interacts with and promotes synaptic accumulation of the βPix guanine nucleotide exchange factor for Rac1 and Cdc42. *J. Biol. Chem.* **278**, 19220-19229.

Penzes, P., Johnson, R. C., Sattler, R., Zhang, X., Huganir, R. L., Kambampati, V., Mains, R. E. and Eipper, B. A. (2001). The neuronal Rho-GEF kalirin-7 interacts with PDZ domain-containing proteins and regulates dendritic morphogenesis. *Neuron* **29**, 229-242.

Penzes, P., Beeser, A., Chernoff, J., Schiller, M. R., Eipper, B. A., Mains, R. E. and

Huganir, R. L. (2003). Rapid induction of dendritic spine morphogenesis by trans-synaptic ephrinB-EphB receptor activation of the Rho-GEF kalirin. *Neuron* **37**, 263-274.

Purpura, D. P. (1974). Dendritic spine "dysgenesis" and mental retardation. *Science* **186**, 1126-1128.

Ramakers, G. J. (2002). Rho proteins, mental retardation and the cellular basis of cognition. *Trends Neurosci.* **25**, 191-199.

Ropers, H. H. and Hamel, B. C. (2005). X-linked mental retardation. *Nat. Rev. Genet.* **6**, 46-57.

Stoppini, L., Buchs, P. A. and Muller, D. (1991). A simple method for organotypic cultures of nervous tissue. *J. Neurosci. Methods* **37**, 173-182.

Tashiro, A. and Yuste, R. (2004). Regulation of dendritic spine motility and stability by Rac1 and Rho kinase: evidence for two forms of spine motility. *Mol. Cell Neurosci.* **26**, 429-440.

Weickert, S., Ray, A., Zoidl, G. and Dermietzel, R. (2005). Expression of neural connexins and pannexin1 in the hippocampus and inferior olive: a quantitative approach. *Brain Res. Mol. Brain Res.* **133**, 102-109.

Zhang, H., Webb, D. J., Asmussen, H. and Horwitz, A. F. (2003). Synapse formation is regulated by the signalling adaptor GIT1. *J. Cell Biol.* **161**, 131-142.

Zhang, H., Webb, D. J., Asmussen, H., Niu, S. and Horwitz, A. F. (2005). A GIT1/PIX/Rac/PAK signalling module regulates spine morphogenesis and synapse formation through MLC. *J. Neurosci.* **25**, 3379-3388.